Modified magnetohydrodynamic waves in a current sheet in space

M. Yamauchi
Swedish Institute of Space Physics, Box 812, S-98128 Kiruna, Sweden.

A. T. Y. Lui
JHU/APL, Laurel, MD 20723-6099, USA.
(accepted 25 August 1997)

Large-scale coherent motions of a current sheet such as flapping or tearing of the entire current sheet are studied. The basic magnetohydrodynamic (MHD) equations are integrated over the thickness of the current sheet, and linear analysis is applied to obtain the modified dispersion relations for the MHD fast, Alfvén, and the slow waves under non-zero background cross-sheet current. The dispersion relation for the fast and slow modes contains an imaginary part, because energy is exchanged between the wave and the background sheet current. A short-wavelength MHD slow wave propagating against/along the magnetic tension force is unstable/stable, whereas the situation is reversed for the MHD fast waves. For a thin current sheet (long-wavelength limit), the MHD slow wave becomes stagnant and very unstable, whereas the MHD fast wave propagates slowly and its stability depends on the strength of the background current.

52.35.Bj , 52.35.Py , 52.65.Kj , 94.30.Ej

Published in Phys. Plasmas 4, 4382 (copyright 1997 by AIP) http://dx.doi.org/10.1063/1.872600)

I. INTRODUCTION

One important issue in space plasma physics is the dynamics of a current sheet such as the terrestrial plasma sheet, Jovian current disk, heliospheric current sheets, filaments of the solar chromosphere and corona, and bow shocks and magnetopauses of the planetary magnetospheres. The density and pressure of plasma inside these current sheets are normally much higher than those outside them[1], and hence many current sheets in space are called plasma sheets. This topic could also be important for dense plasma inside plasma laboratories or stars[2,3,4]. However, basic processes such as the behavior of large-scale magnetohydrodynamic (MHD) waves inside the current sheet have not yet been well understood. Most of the wave studies have been carried out linearly or quasi-linearly when the background magnetic field is uniform or very weakly bent[5], but not when it is strongly bent because of difficulties in modeling.

Let us consider, for example, the terrestrial plasma sheet. In the simplest configuration, it is represented by a duskward background current $J_y(x)\hat{\mathbf{y}}$ in a northward background magnetic field $B_z(x)\hat{\mathbf{z}}$ as shown in Figure 1a (x sunward, y duskward, and z northward). This current makes B_x (sunward pointing background magnetic field) non-uniform in the z direction even though the current outside of the plasma sheet is nearly zero[6]. It is not easy even to linearize the basic MHD equations in such a configuration.

Analogy of the linear MHD waves in uniform media may help to predict the large-scale dynamics of the entire current sheet. We expect three basic large-scale coherent motions corresponding to the MHD fast, Alfvén, and slow waves, as shown in Figure 2. The Alfvén mode (Figure

2a) preserves the strength of the magnetic and plasma pressures because it is an incompressional mode, while these pressures vary in-phase and out-of-phase for the MHD fast and slow modes, respectively. The increase of B_x caused by the fluctuations of cross-sheet current must be located at the plasma density maximum/minimum for the fast/slow modes (Figures 2b/2c).

These predictions are not bad for space plasma. Ulysses observations of magnetic and plasma disturbances in the Jovian current disk suggest the existence of the tearing-like motions with a period of 1.9 hours[7] in addition to the 11-hour period flapping motion due to the Jovian rotation[8]. Both Hyakutake and Hale-Bopp comets clearly demonstrated the existence of tearing- and/or flapping-like structures in the plasma tail while the dust tail does not have such structures. The planetary bow shock and magnetopause are also well known to have wave-like motion[9]. Propagation of the tearing motion of the terrestrial plasma sheet has been proposed to explain the triggering of magnetic reconnection and plasmoid formation shortly after a substorm onset at the inner edge of the plasma sheet[10,11].

Another difficulty is the kinetic effect because the current sheets in space are only several ion gyroradii thick and filled with non-Maxwellian plasma. If this effect is significant, the MHD treatment is questionable and Figure 2's predictions are no longer useful. Fortunately, MHD has been successful in describing the approximate configuration of the current sheets such as the terrestrial magnetopause[12]. Therefore, we may probably use MHD as long as we consider large-scale motions.

If Figure 2's predictions are correct, we may make the following simplifications. *1.* We may assume $\partial/\partial y = 0$ strictly for background and disturbed quantities. We may also assume duskward background field $B_y = 0$. *2.* The motion decays outside the current sheet. Since $P' \gg P'_e$ in Figure 1a, we may make the plane wave approximation with the wave normal pointing the x direction. *3.* For the same reason, we may integrate the physical quantities over the thickness of the current sheet as shown in Figure 1b.

These simplifications enable us to derive appropriate basic equations for linear studies of large-scale motions of a current sheet. This is the first purpose of this paper. The second purpose is to obtain the dispersion relation for the predicted large-scale coherent motion as shown in Figure 2. We ignore the kinetic effect for these studies.

II. THICKNESS INTEGRATION

Integration of the current sheet over its thickness as shown in Figure 1b is not simple unless the background magnetic field is uniform such as in the ionosphere[13] because otherwise the magnetic tension force caused by the bending of the geomagnetic field[6] is not negligible. Therefore, we employ the following assumptions:

(a) $\acute{\rho}(z=h) \ll \acute{\rho}(z=0)$

(b) $\acute{P}(z=h) \ll \acute{P}(z=0)$

(c) $|\frac{\partial \acute{u}_x}{\partial z}| \ll |\frac{\langle \acute{u}_x \rangle}{h}|$

(d) $\acute{u}_z \ , \ \acute{u}_y \ll \langle \acute{u}_x \rangle$

(e) $|\frac{\partial B_z}{\partial z}| \ll |\frac{\langle B_z \rangle}{h}|$

(g) $r_g < h \ll L$

where $\acute{\rho}$, $\acute{\mathbf{u}}_{x,y}$, and $\acute{P}$ are mass density, convection velocity along the equatorial plane, and pressure; h is the thickness of the current sheet outside of which the plasma density is negligibly small; L is the scale length along the current sheet; r_g is the ion Larmor radius; and the quantities within the bracket are averaged over the thickness, e.g., $\langle \acute{u}_{x,y} \rangle = \int \acute{u}_{x,y} dz/h$, etc.

These assumptions are quite reasonable in the terrestrial plasma sheet[1,14] although assumption (c) could be invalid when the flow speed in the plasma sheet boundary layer is much faster than that in the central plasma sheet. The effect of such north-south velocity shear should be studied by a different method. The last assumption is the necessary condition for the MHD approximation, but the sufficient conditions to ignore the kinetic effect in space plasma is still an open question. So, we simply assume the validity of MHD in this paper.

The thickness-integrated mass density (ρ), momentum ($\rho \mathbf{u}_{x,y}$, F_z), pressure (P), and electric current ($\mathbf{I}$) are defined as

$$(\rho \ , \ \rho \mathbf{u}_{x,y} \ , \ P \ , \ \mathbf{I}_{x,y}) \equiv \int_{-h}^{+h} (\acute{\rho} \ , \ \acute{\rho} \acute{\mathbf{u}}_{x,y} \ , \ \acute{P} \ , \ \acute{\mathbf{J}}_{x,y}) dz$$

$$F_z \equiv [\acute{\rho} \acute{u}_z]_{-h}^{+h}$$

where $F_z \propto \rho/h$ is a small mass flux escaping (or supply for minus sign) from the current sheet in the z direction. We also define $B_z \equiv \langle \acute{B}_z \rangle$, $B_{x,y} \equiv [\acute{B}_{x,y}]_{z=h}$, and $I_z \equiv hJ_z \equiv h[\acute{J}_z]_{z=h}$. Since both $\acute{B}_{x,y}$ and $\acute{J}_z$ are zero at the $z = 0$ plane, their z dependency must be very similar to each other.

We now integrate the basic MHD equations over the thickness. The thickness-integrated continuity equation is:

$$\begin{aligned} \frac{\partial}{\partial t}\rho &= \int_{-h}^{+h} \frac{\partial \acute{\rho}}{\partial t} dz = -\int_{-h}^{+h} \nabla \cdot (\acute{\rho} \acute{\mathbf{u}}) dz \\ &= -\nabla_{x,y} \cdot \int_{-h}^{+h} \acute{\rho} \acute{\mathbf{u}}_{x,y} dz - \int_{-h}^{+h} \frac{\partial}{\partial z} (\acute{\rho} \acute{u}_z) dz \\ &= -\nabla_{x,y} \cdot (\rho \mathbf{u}_{x,y}) - F_z \end{aligned} \tag{1}$$

The thickness-integrated momentum equations are:

$$\begin{aligned} \frac{\partial}{\partial t}(\rho u_x) \cong &-\nabla_{x,y} \cdot (\rho u_x \mathbf{u}_{x,y}) - [\acute{\rho} \acute{u}_x \acute{u}_z]_{-h}^{+h} - \frac{\partial P}{\partial x} \\ &+ B_z \int_{-h}^{+h} \acute{J}_y dz - \int_{-h}^{+h} \acute{J}_z \acute{B}_y dz \end{aligned}$$

$$\cong -\nabla_{x,y}(\rho u_x \mathbf{u}_{x,y}) - u_x F_z - \frac{\partial P}{\partial x} + I_y B_z - \alpha_A I_z B_y \quad (2)$$

$$\frac{\partial}{\partial t}(\rho u_y) \cong -\nabla_{x,y}(\rho u_y \mathbf{u}_{x,y}) - u_y F_z - I_x B_z + \alpha_A I_z B_x \quad (3)$$

$$\frac{\partial}{\partial t}(\acute{\rho}\acute{u}_z) \cong -\frac{\partial}{\partial x}(u_x \acute{\rho}\acute{u}_z) - \frac{\partial}{\partial y}(u_y \acute{\rho}\acute{u}_z) - \frac{\partial}{\partial z}(\acute{\rho}\acute{u}_z^2) - \frac{\partial \acute{P}}{\partial z} + \acute{J}_x \acute{B}_y - \acute{J}_y B_x$$

$$\frac{\partial}{\partial t}F_z \cong -\nabla_{x,y}(F_z \mathbf{u}_{x,y}) - \alpha_p \frac{P}{h^2} - \alpha_c \frac{I_y B_x}{h} - \alpha_L \frac{I_x B_y}{h} \quad (4)$$

where $\alpha_A = O(1)$ is an integral constant for $\int_{-h}^{+h} \acute{J}_z^2 dz$, i.e., $\alpha_A = 2/(2n+1)$ if $\acute{J}_z \propto z^n$; and we assumed the same z dependence for $\acute{B}_{x,y}$ and $\acute{J}_z$. The other integral constants are $\alpha_p = O(1)$ ($= \gamma^2 h^2/2d^2$ if $\acute{P} \propto \mathrm{e}^{-\gamma|z|/d}$), $\alpha_c = O(1)$ ($\cong 0.14h/d$ if $\acute{J}_y \propto \mathrm{e}^{-|z|/d}$), and $\alpha_L = O(1)$.

The z component induction equation is:

$$\frac{\partial}{\partial t}B_z = \langle \frac{\partial}{\partial x}(\acute{\mathbf{u}} \times \acute{\mathbf{B}})_y \rangle - \langle \frac{\partial}{\partial y}(\acute{\mathbf{u}} \times \acute{\mathbf{B}})_x \rangle \cong -\nabla_{x,y}(B_z \mathbf{u}_{x,y}) + \eta \nabla_{x,y}(\frac{F_z \mathbf{B}_{x,y}}{\rho_0}) \quad (5)$$

where $\eta = O(1)$ is the integral constant for $\int_{-h}^{+h} \acute{u}_z \acute{\mathbf{B}}_{x,y} dz$. To close the above equation system, we need to express $\mathbf{I}$ in terms of $\mathbf{E}$ and/or $\mathbf{B}$.

A simple application of the plain wave assumption to the Ampere's law yields:

$$\mu_0 I_z = -\frac{\partial}{\partial x}(2hB_y) \quad (6)$$

$$\mu_0 I_y = -\frac{\partial}{\partial x}(2hB_z) \quad (7)$$

Eq. (6) is fine, but Eq. (7) is wrong because Eq. (7) means an increase of field energy when the cross-tail current I_y is reduced. Therefore, we have to integrate the original Ampere's law over the z direction.

$$\mu_0 I_y = \int_{-h}^{+h} (\frac{\partial \acute{B}_x}{\partial z} - \frac{\partial \acute{B}_z}{\partial x}) = [\acute{B}_x]_{-h}^{+h} - \frac{\partial}{\partial x}(2hB_z)$$

where B_x can be expressed by u_x according to the frozen-in relation illustrated in Figure 3:

$$\frac{\delta x}{h} = \frac{\delta B_x}{B_z} = \frac{\delta [\acute{B}_x]_{z=0}^{z=h}}{B_z}$$

or

$$\mu_0 \delta I_y = 2B_z \frac{\delta x}{h} - \frac{\partial}{\partial x}(2h\delta B_z)$$

where δx is the relative displacement of the plasma between $z = 0$ and $z = h$. Using this relation, we finally obtain

$$\frac{dI_y}{dt} = \frac{2B_z}{\mu_0 h}\frac{d(\delta x)}{dt} - \frac{2h}{\mu_0}\frac{\partial^2 B_z}{\partial x \partial t} \tag{8}$$

where $d(\delta x)/dt$ is the deviation from the background convection.

III. BASIC EQUATIONS

Let us summarize the basic Eqs. (1)-(6), and (8) under the strict $\partial/\partial y = 0$ assumption.

$$\frac{\partial}{\partial t}\rho = -\frac{\partial}{\partial x}(\rho u_x) - F_z \tag{9a}$$

$$\frac{\partial}{\partial t}(\rho u_x) = -\frac{\partial}{\partial x}(\rho u_x^2) - u_x F_z - \frac{\partial P}{\partial x} + I_y B_z \tag{9b}$$

$$\frac{\partial}{\partial t}(\rho u_y) = -\frac{\partial}{\partial x}(\rho u_y u_x) + \alpha_A I_z B_x - I_x B_z - u_y F_z \tag{9c}$$

$$\frac{\partial}{\partial t}F_z = -\frac{\partial}{\partial x}(u_x F_z) - \alpha_p \frac{P}{h^2} - \alpha_c \frac{I_y B_x}{h} - \alpha_L \frac{I_x B_y}{h} \tag{9d}$$

$$\delta B_x = \frac{B_z}{h}\delta x \tag{9e}$$

$$\frac{\partial}{\partial t}B_z = -\frac{\partial}{\partial x}(B_z u_x) + \eta \frac{\partial}{\partial x}\left(\frac{h B_x F_z}{\rho_0}\right) \tag{9f}$$

$$\frac{\partial}{\partial t}B_y = B_x \frac{\partial}{\partial x}u_y - \frac{\partial}{\partial x}(B_y u_x) \tag{9g}$$

$$\frac{d}{dt}I_y = \frac{2B_z}{\mu_0 h}\frac{d(\delta x)}{dt} - \frac{2h}{\mu_0}\frac{\partial^2 B_z}{\partial x \partial t} \tag{9h}$$

$$I_z = \frac{2h}{\mu_0}\frac{\partial}{\partial x}B_y \tag{9i}$$

where $0 < \alpha \leq 1$ is the integral constant. To close the above system of equations under given background convection u_0 (i.e., $u_x = u_0 + d(\delta x)/dt$), we need the Ohm's law to express I_x ($= -[\acute{B}_y]_{-h}^{+h}/\mu_0$). Although the I_x term becomes important in Eq. (9c) when we consider strong background convection, it can be ignored in the linear analyses of a subsonic flow[15,16]. Therefore, we do not need to obtain the expression for I_x.

Eq. (9) must be linearized for wave mode analyses. The zero-order and first-order magnetic fields are expressed as $\mathbf{B} = (B_x, 0, B_z)$ and $\mathbf{b} = (b_x, b_y, b_z)$, where we include non-zero $B_x = \mu_0 I_0/2$ and non-zero background convection $u_0\hat{\mathbf{x}}$. The zero-order equations are then summarized as:

$$\frac{\partial}{\partial x}(\rho_0 u_0) = 0 \tag{10a}$$

$$\frac{\partial}{\partial x}(B_z u_0) = 0 \tag{10b}$$

$$\frac{1}{\rho_0}\frac{\partial P_0}{\partial x} = \frac{2B_x B_z}{\mu_0 \rho_0} - u_0 \frac{\partial u_0}{\partial x} \tag{10c}$$

where the present approximation is valid only for subsonic flows.

The z component momentum equation requires gradient of P_0 to be balanced with $I_0 B_x$ in the z direction, but it does not restrict the x dependence of P_0. Therefore, Eq. (10) has a non-trivial solution.

IV. LINEAR ANALYSES

The first order equations for the perturbations are obtained by subtracting Eq. (10) from Eq. (9). We have

$$\frac{D}{Dt}\rho = -\rho_0 \frac{\partial u_x}{\partial x} - F_z \tag{11a}$$

$$\rho_0 \frac{D}{Dt} u_x = -C_S^2 \frac{\partial \rho}{\partial x} - u_0 F_z + I_y B_z + \frac{2 B_x b_z}{\mu_0} \tag{11b}$$

$$\frac{D}{Dt} F_z = -\alpha_p \frac{P}{h^2} - \alpha_c \frac{B_x I_y}{h} - \alpha_c \frac{2 B_x}{\mu_0 h} b_x \tag{11c}$$

$$\frac{D}{Dt} b_x = \frac{B_z}{h} u_x \tag{11d}$$

$$\frac{D}{Dt} b_z = -B_z \frac{\partial u_x}{\partial x} + (\frac{\eta h B_x}{\rho_0}) \frac{\partial F_z}{\partial x} \tag{11e}$$

$$\frac{D}{Dt} I_y = \frac{2 B_z}{\mu_0 h} u_x - \frac{2h}{\mu_0} \frac{\partial^2 b_z}{\partial x \partial t} \tag{11f}$$

for the magnetosonic mode ($u_y = 0$), and

$$(\frac{D}{Dt})^2 u_y = \alpha_A V_{Ax}^2 \frac{\partial^2}{\partial x^2} u_y - B_z \frac{D}{Dt} I_x \tag{12a}$$

$$(\frac{D}{Dt})^2 F_z = \eta \alpha_c V_{Ax}^2 \frac{\partial^2}{\partial x^2} F_z \tag{12b}$$

for the incompressional mode ($\delta x = 0$), where $D/Dt = \partial/\partial t + u_0 \partial/\partial x$ is the Lagrange time derivative which causes the Doppler shift effect, $V_A = B\sqrt{2h/\mu_0 \rho_0}$ is the Alfvén speed, $C_S = \sqrt{(\partial P/\partial \rho)_{ad}}$ is the sound speed, the subscript "ad" denotes adiabatic compression, and the coupling terms from the magnetosonic mode ($\delta x \neq 0$) to the incompressional mode ($u_y \neq 0$) are ignored whereas there is no coupling from the incompressional mode ($u_y \neq 0$) to the magnetosonic mode ($\delta x \neq 0$) in the linear limit. Solution (12b) corresponds to the flapping motion in the z direction illustrated in Figure 2a, whereas solution (12a) is a slip of the current sheet in the y direction without changing the location and density of the current sheet. Since the $I_x B_z$ term in Eq. (9c) is small compared to the $I_z B_x$ term under the $\partial/\partial y = 0$ assumption[15], the last term in Eq. (12a) can be ignored and both the incompressional solutions become the same as that for the Alfvén mode in uniform media[5]. We hereafter consider the magnetosonic mode only.

Eq. (11) for the magnetosonic mode becomes:

$$(\frac{D^2}{Dt^2} - C_S^2 \frac{\partial^2}{\partial x^2}) u_x =$$

$$V_{Az}^2\frac{\partial^2}{\partial x^2}u_x - \frac{\eta V_{Ax}V_{Az}h}{\rho_0}\frac{\partial^2}{\partial x^2}F_z - \frac{V_{Ax}V_{Az}}{h}\frac{\partial}{\partial x}u_x$$
$$+\frac{\eta V_{Ax}^2}{\rho_0}\frac{\partial}{\partial x}F_z + \frac{V_{Az}^2}{h^2}u_x - \frac{u_0}{\rho_0}\frac{D}{Dt}F_z + \frac{C_S^2}{\rho_0}\frac{\partial}{\partial x}F_z \quad (13)$$

$$\frac{D^2F_z}{Dt^2} = \alpha_p\frac{C_S^2\rho_0}{h^2}\frac{\partial u_x}{\partial x} + \alpha_p\frac{C_S^2}{h^2}F_z + \eta\alpha_c V_{Ax}^2\frac{\partial^2 F_z}{\partial x^2}$$
$$-\alpha_c\frac{V_{Ax}V_{Az}\rho_0}{h}(\frac{\partial^2 u_x}{\partial x^2} + \frac{2u_x}{h^2}) \quad (14)$$

There are seven terms on the right hand side of Eq. (13). The first two terms and the fifth term represent the contributions from the magnetic pressure through δI_y, the third and fourth terms represent the energy loss from the wave through b_z during the compression, and the last two terms represent the momentum and mass transfers from u_z to u_x. The fifth term brings the dispersion effect into the system, making the wave signature complicated, e.g., converting the b_z signature from monopolar to bipolar. Right hand side of Eq. (14) is attributed to the pressure gradient force (terms with α_p) and the $J\times B$ force (terms with α_c). The second term causes dispersion whereas the last term inside the bracket causes dissipation or instability due to the energy coupling between the wave and the cross-sheet current.

Now, we take the Foureir analyses. Assuming the perturbed quantities $\propto \exp[-i\omega t + ikx]$, Eqs. (13) and (14) become:

$$[\omega_\delta^2 - k^2(C_S^2 + V_{Az}^2) - ik\frac{V_{Ax}V_{Az}}{h} + \frac{V_{Az}^2}{h^2}]u_x$$
$$= -[i\omega_\delta\frac{u_0}{\rho_0} + k^2\frac{\eta V_{Ax}V_{Az}h}{\rho_0} + ik\frac{\eta V_{Ax}^2 + C_S^2}{\rho_0}]F_z$$

and

$$[\omega_\delta^2 - k^2\eta\alpha_c V_{Ax}^2 + \alpha_p\frac{C_S^2}{h^2}]F_z$$
$$= -[k^2\alpha_c\frac{V_{Ax}V_{Az}\rho_0}{h}(1 - \frac{2}{k^2h^2}) + ik\alpha_p\frac{C_S^2\rho_0}{h^2}]u_x$$

where $\omega_\delta = \omega - ku_0$ is the Doppler-shifted frequency. Combining these equations for subsonic u_0, we have:

$$[\frac{\omega_\delta^2}{k^2} - (C_S^2 + V_{Az}^2) - i\frac{V_{Ax}V_{Az}}{kh} + \frac{V_{Az}^2}{k^2h^2}]$$
$$\times [\frac{\omega_\delta^2}{k^2} - \eta\alpha_c V_{Ax}^2 + \alpha_p\frac{C_S^2}{k^2h^2}]$$
$$\cong [\eta V_{Ax}V_{Az} + i\frac{\eta V_{Ax}^2 + C_S^2}{kh}]$$
$$\times [\alpha_c V_{Ax}V_{Az}(1 - \frac{2}{k^2h^2}) + i\alpha_p\frac{C_S^2}{kh}] \quad (15)$$

Unlike the MHD dispersion relation in uniform media, Eq. (15) includes the imaginary part which determines the evolution of the wave. For example, a wave propagating toward the $-x$ ($+x$) direction, i.e., against (along)

the magnetic tension force grows (decays) if the solution satisfies $\omega_i/k < 0$. The non-zero horizontal wave length compared to the thickness of the current sheet is solely responsible for the dispersion because the imaginary unit always appears as $i(kh)^{-1}$ or its power in Eq. (15). Therefore, the wave behavior must be quite different between for short-wavelength ($r_g \ll 1/k < h$) and long-wavelength ($1/k > h > r_g$) cases.

For a thick current sheet ($r_g \ll 1/k < h$), dispersion relation (15) must become similar to that for the ordinary MHD waves in uniform media. To see it, we assume real k vector and set $\omega_\delta = \omega_r + i\omega_i$. The real part of the equation becomes:

$$\begin{aligned}
&(V_{ph}^2)^2 - C_F^2 V_{ph}^2 + \eta\alpha_c V_{Ax}^2 C_S^2 \\
&= -\frac{(\alpha_p C_S^2 + V_{Az}^2)}{k^2h^2} V_{ph}^2 - \frac{(\alpha_p C_S^2 + \alpha_c V_{Az}^2)\eta V_{Ax}^2}{k^2h^2} \\
&\quad + \frac{\alpha_p C_S^2 V_{Az}^2}{k^2h^2} - \frac{\alpha_p C_S^2 V_{Az}^2}{k^4h^4} \\
&\quad - \frac{2\omega_i}{\omega_r}\frac{V_{Ax}V_{Az}}{kh} V_{ph}^2 + O(\frac{\omega_i^2}{\omega_r^2}) V_{ph}^4
\end{aligned} \tag{16}$$

where $C_F = \sqrt{C_S^2 + V_{Az}^2 + \eta\alpha_c V_{Ax}^2}$ is the MHD fast speed, $V_{ph} = \omega_r/k$ is the phase velocity, $O()$ denotes the order of magnitude, and we assumed $\omega_r \gg \omega_i$. The left hand side of (16) is very similar to the ordinary dispersion relation for the magnetosonic waves in uniform media[5]. The right hand side of (16) is the correction due to the finite thickness ($kh \neq \infty$) of the current sheet.

The imaginary part of (15) becomes

$$\begin{aligned}
&[2V_{ph}^2 - C_F^2 + \frac{V_{Az}^2 + \alpha_p C_S^2}{k^2h^2}]\frac{2\omega_i khV_{ph}^2}{\omega_r V_{Ax}V_{Az}} = \\
&V_{ph}^2 + (\eta\alpha_p + \alpha_c)C_S^2 + \frac{\alpha_p C_S^2 - 2\alpha_c C_S^2 - 2\eta\alpha_c V_{Ax}^2}{k^2h^2}
\end{aligned}$$

Especially for a thick current sheet ($1/k \ll h$), it becomes

$$\frac{\omega_i}{\omega_r} = \pm\frac{V_{Ax}V_{Az}}{2khV_{ph}^2}[\frac{V_{ph}^2 + (\eta\alpha_p + \alpha_c)C_S^2}{\sqrt{C_F^4 - 4\eta\alpha_c V_{Ax}^2 C_S^2}} + O(\frac{1}{k^2h^2})] \tag{17}$$

where

$$V_{ph}^2 = \frac{C_F^2 \pm \sqrt{C_F^4 - 4\eta\alpha_c V_{Ax}^2 C_S^2}}{2} O(\frac{C_F^2}{k^2h^2})$$

and the positive (negative) sign is for the MHD fast (slow) mode. Inside the large bracket of Eq. (17) is nearly unity because the sound speed is normally faster than the Alfvén speed inside the current sheet. Therefore, the growth or decay rate ω_i is nearly proportional to the finite cross-sheet current I_0 ($\propto B_x \propto V_{Ax}$): the MHD slow wave grows when travelling against the magnetic tension force whereas MHD fast wave grows when travelling along the magnetic tension force for the short-wavelength limit ($r_g \ll 1/k \ll h$). The free energy of this instability comes from the sheet current.

This MHD instability causes a coherent tearing motion as shown in Figure 2, but is not the same as the ordinary microscopic tearing mode instability. The latter requires the dissipation of the electric current as the non-MHD effect[17] whereas the former requires only the energy conversion from the magnetic field to the bulk motion. Therefore, the growth rate given by Eq. (17) is different from that for the ordinary microscopic tearing mode instability[17].

Let us move to a thin current sheet case ($1/k > h > r_g$). Note that our formulation is valid only when the kinetic effect can be neglected. Since one may no longer assume $\omega_r > \omega_i$, we start from Eq. (15) under $kh \ll 1$ assumption.

$$(h^2\omega_\delta^2)^2 + h^2\omega_\delta^2[\alpha_p C_S^2 + V_{Az}^2 - ikhV_{Ax}V_{Az}] + \alpha_p C_S^2 V_{Az}^2 + ikhV_{Ax}V_{Az}[\eta\alpha_c V_{Ax}^2 + (2\alpha_c - \alpha_p)C_S^2] = O(k^2h^2C_S^4)$$

or

$$[h^2\omega_\delta^2 + \alpha_p C_S^2 - ikhV_{Ax}V_{Az}\xi_s] \times [h^2\omega_\delta^2 + V_{Az}^2 - ikhV_{Ax}V_{Az}\xi_f] = O(k^2h^2C_S^4) \quad (18)$$

where

$$\xi_s = \frac{2\alpha_c C_S^2 + \alpha_c \eta V_{Ax}^2}{\alpha_p C_S^2 - V_{Az}^2} > 0$$

$$\xi_f = \frac{(\alpha_p - 2\alpha_c)C_S^2 - \alpha_c\eta V_{Ax}^2 - V_{Az}^2}{\alpha_p C_S^2 - V_{Az}^2}$$

and the sign of ξ_f depends on the strength of the sheet current because $\alpha_p - 2\alpha_c$ is normally positive.

The solutions for Eq. (18) are:

$$h\omega_\delta = \pm i\sqrt{\alpha_p}C_S[1 - ikh\frac{\xi_s V_{Ax}V_{Az}}{2\alpha_p C_S^2} + O(k^2h^2)] \quad (19a)$$

or

$$\pm iV_{Az}[1 - ikh\frac{\xi_f V_{Ax}}{2V_{Az}} + O(k^2h^2)] \quad (19b)$$

The first solution (19a) corresponds to the MHD slow mode with $|\omega_r| < |\omega_i|$, i.e., a quick growth/decay under slow propagation along/against the magnetic tension force in the plasma rest frame (moving with u_0). The solution is somewhat similar to the growth rate of the ordinary microscopic tearing mode instability but different from it by a factor of $\sqrt{r_{ge}/h}$, where r_{ge} is the electron Larmor radius[17]. The other solution (19b) corresponds to the MHD fast mode. If $C_S > V_{Ax}$, the wave quickly grows/decays when propagating slowly along/against the magnetic tension force, which is the same as the case for short-wavelength limit. However, this is reversed if the current layer is strong enough to satisfy $C_S < V_{Ax}$.

V. TERRESTRIAL PLASMA SHEET

Typical values for the terrestrial plasma sheet[1,6,14] are $B_z \cong 1.5$ nT, $B_x \cong 5$ nT, plasma density $\cong 0.3\,\mathrm{cm}^{-3}$, and

$T = 0.5 \sim 3\times10^7$ K. From these values we have $V_{Az} \cong 50$ km/s, $V_{Ax} \cong 200$ km/s, and $C_S = 200 \sim 500$ km/s within a factor of 3 in accuracy. Assuming $\alpha_A = 0.4$, $\alpha_p = 0.5$, $\alpha_c = 0.15$, and $\eta = 0.3$ (i.e., $\xi_s = 0.7 \sim 0.6$ and $\xi_f = 0.2 \sim 0.4$), we have approximately

$$V_{ph} \text{ (fast)} \cong C_S = 200 \sim 500 \text{ km/s}$$
$$h|\omega_i| \text{ (fast)} = 15 \sim 30 \text{ km/s} \tag{20a}$$
$$V_{ph} \text{ (slow)} \cong 0.8V_{Az} \cong 40 \text{ km/s}$$
$$h|\omega_i| \text{ (slow)} \cong 35 \text{ km/s} \tag{20b}$$

for very short-wavelength limit ($1/k \ll h$), and

$$h|\omega_i| \text{ (fast)} \cong 50 \text{ km/s} \gg V_{ph} \text{ (fast)} \tag{20c}$$
$$h|\omega_i| \text{ (slow)} = 150 \sim 350 \text{ km/s} \gg V_{ph} \text{ (slow)} \tag{20d}$$

for very long-wavelength limit ($1/k \gg h > r_g$). Since the thickness of the terrestrial plasma sheet is about a few Earth radius ($h \cong 5000 - 10000$ km/s), (20b) means a growth time of about 5 minutes. This cannot be ignored compared to the travel time of the MHD slow wave from the inner edge of the plasma sheet to the near-Earth magnetic neutral line[10].

In the terrestrial plasma sheet, the current density gradually changes in the x direction, and this effect is illustrated in Figure 4. As a result, the growing perturbed b_z may exceed the background B_z. If the original perturbations of the plasma pressure and the magnetic pressure is out-of-phase (slow mode), they may become in-phase (fast mode) at this point. The above estimation supports this scenario. Then u_x must exceed the MHD fast velocity according to the MHD fast mode relation ($b_z/B_z \cong u_x/C_F$). Together with the density increase expected from the mode relation, we naturally predict a clear plasmoid signature with an attached slow shock, as is observed by the Geotail satellite[18]. Thus, the plasmoid can be formed as the result of the tailward propagation of current disruption.

VI. CONCLUSIONS

We studied coherent motions of a current sheet. Using linear analyses on the thickness-integrated MHD equations with non-zero background sheet current, we obtained dispersion relations for the MHD fast, Alfvén, and slow waves. The present study does not include the kinetic effect nor the background velocity shear in the z direction. Unlike the ordinary MHD dispersion relations in a uniform medium, the dispersion relation includes an imaginary part, causing growth or decay of the waves. The growth rate is nearly proportional to the total cross-tail current, representing energy coupling between the wave and the cross-tail current. A short-wavelength MHD slow wave propagating against/along the magnetic tension force is unstable/stable, whereas wave becomes stagnant and very unstable in the long-wavelength limit or a very thin current sheet. The stability of the MHD fast wave depends on the strength of the sheet current.

ACKNOWLEDGMENTS

We thank V. M. Vasyluinas at MPAe, Germany for valuable comments. The effort of ATYL was supported by the National Science Foundation Grant ATM9622080 to the Johns Hopkins University Applied Physics Laboratory.

---

[1] G. K. Parks, M. McCarthy, R. J. Fitzenreiter, J. Etcheto, K. A. Anderson, T. E. Eastman, L. A. Frank, D. A. Gurnett, C. Huang, R. P. Lin, A. T. Y. Lui, K. W. Ogilvie, A. Pedersen, H. Reme, and D. J. Williams, J. Geophys. Res. **89**, 8885-906 (1984).
[2] P. H. Robert, in *Lectures on Solar and Planetary Dynamos*, edited by M. R. E. Proctor and A. D. Gilbert (Cambridge University Press, 1994), p. 1–58.
[3] J.B. Taylor, Phys. Fluids B **5**, 4378–83 (1993).
[4] P. H. Rutherford, Phys. Fluids **16**, 1903–8 (1973).
[5] H. Alfvén and C.-G. Fälthammar, *Cosmical Electrodynamics* (Oxford University Press, 1963), p. 76–100.
[6] D. H. Fairfield, J. Geophys. Res. **91**, 4238–44 (1987).
[7] M. Schulz, J. B. Blake, S. M. Mazuk, A. Balogh, M. K. Dougherty, R. J. Forsyth, E. Keppler, J. L. Phillips, and S. J. Bame, Planet. Space Sci. **41**, 967-75 (1993).
[8] A. Balogh, M. K. Dougherty, R. J. Forsyth, D. J. Southwood, E. J. Smith, B. T. Tsurutani, N. Murphy, and M. E. Burton, Science **257**, 1515-18 (1992).
[9] J. Woch and R. Lundin, J. Geophys. Res. **97**, 1431-47 (1992).
[10] A. T. Y. Lui, J. Geophys. Res. **96**, 1849–56 (1991).
[11] G. Haerendel, Eur. Space Agency Spec. Publ. **335**, 417-20 (1992).
[12] B. U. Ö. Sonnerup and B. G. Ledley, J. Geophys. Res. **79**, 4309-14 (1974).
[13] A. Brekke, J. R. Doupnik, and P. M. Banks, J. Geophys. Res. **79**, 3773–90 (1974).
[14] W. R. Paterson and L. A. Frank, Geophys. Res. Lett. **21**, 2971-4 (1994).
[15] M. Yamauchi, R. Lundin, and A. T. Y. Lui, J. Geophys. Res. **98**, 13523–8 (1993).
[16] M. Yamauchi, Geophys. Res. Lett. **21**, 851–4 (1994).
[17] A. A. Galeev, in *Magnetospheric Plasma Physics*, edited by A. Nishida (Reidel, Dordrecht, 1982), p. 143–96.
[18] S. Machida, T. Mukai, Y. Saito, T. Obara, T. Yamamoto, A. Nishida, M. Hirahara, T. Terasawa, and S. Kokubun, Geophys. Res. Lett. **21**, 2995-8 (1994).

FIG. 1. The current sheet configuration and its simplification. Since we consider MHD waves which decay in both $z = +\infty$ and $z = -\infty$ directions, we attempt to simplify the configuration to a background sheet current in $+y$ direction and a background magnetic field in $+z$ direction.

FIG. 2. Possible coherent motions of thin current sheet. In MHD regime, we expect three modes: fast, Alfvén, and slow.

FIG. 3. The relation between δB_x and the displacement of the plasma in the x direction.

FIG. 4. Illustration of the tailward wave propagation and the launch of a plasmoid or plasma bubbles.

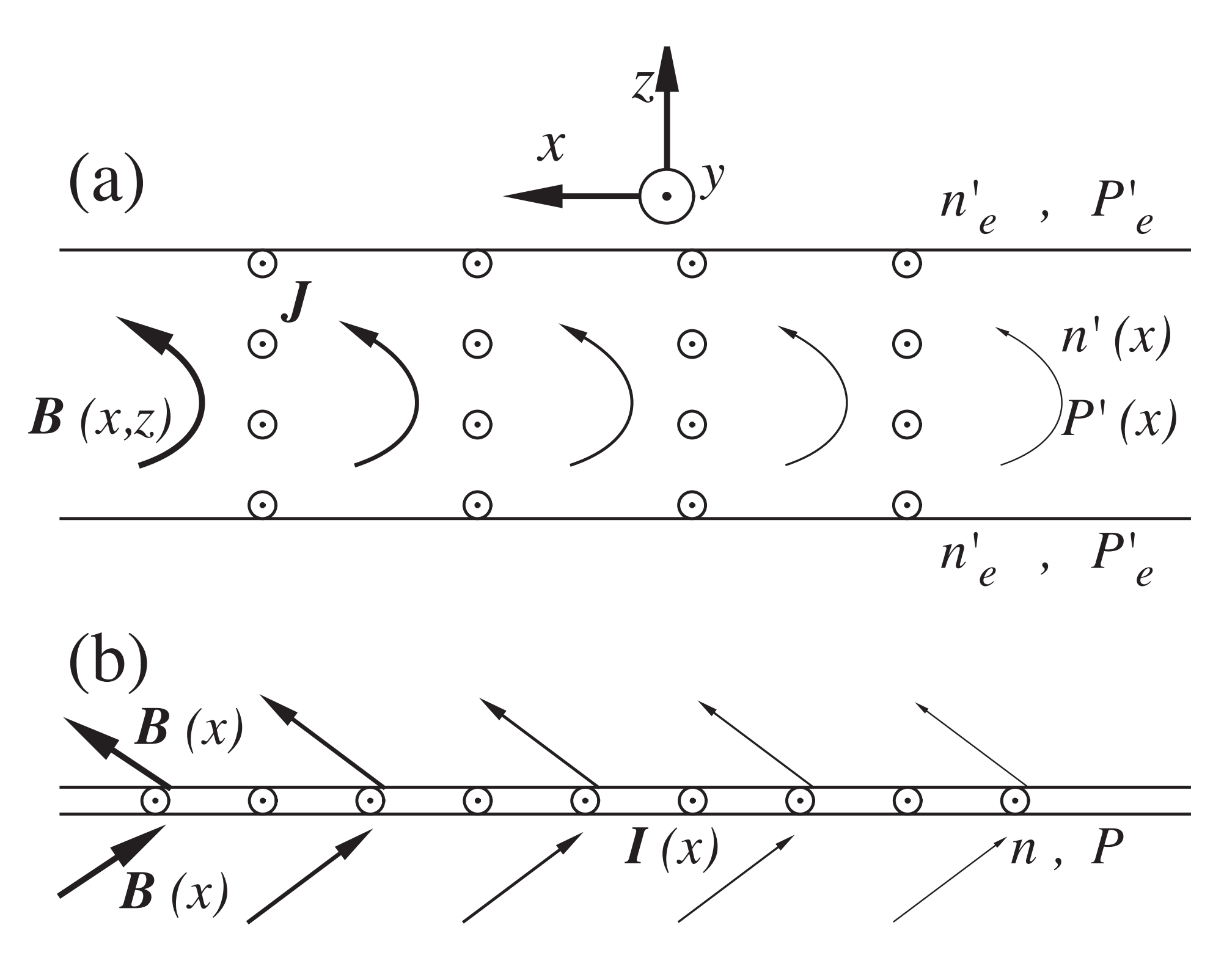
(a)
z
x
y
n'e , P'e
J
B (x,z)
n' (x)
P' (x)
n'e , P'e
(b)
B (x)
B (x)
I (x)
n , P

Alfven Mode (flapping)

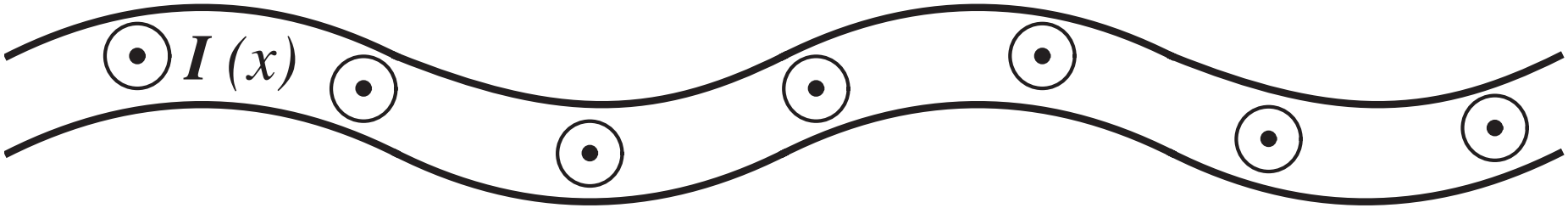

Fast Mode (tearing)

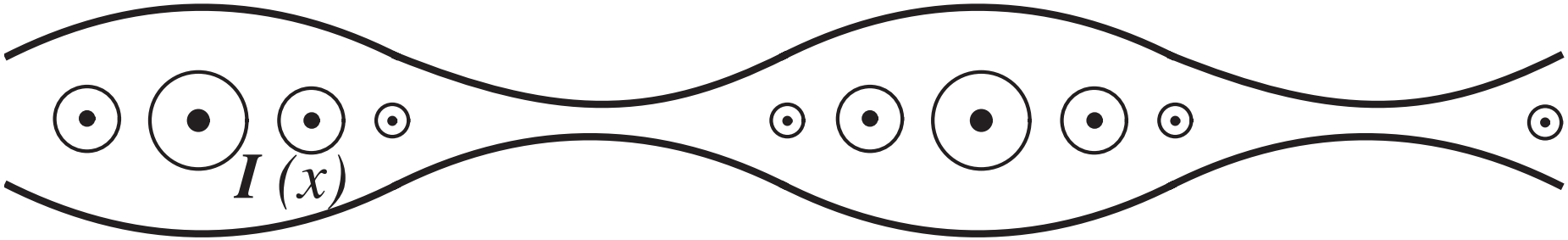

Slow Mode (tearing)

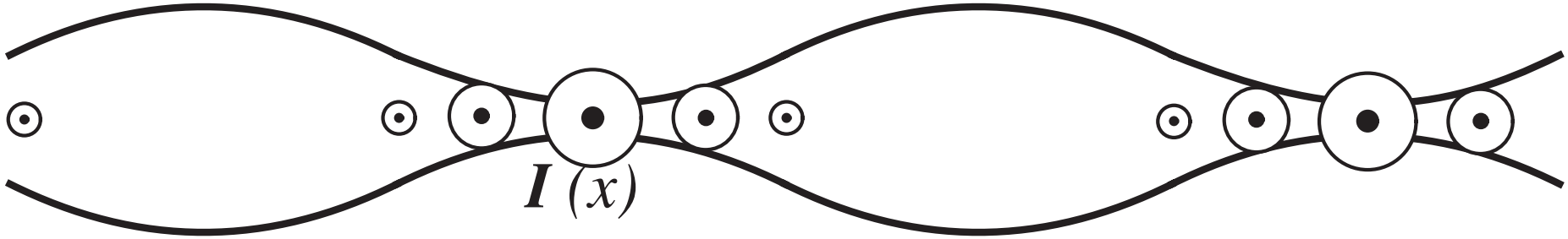

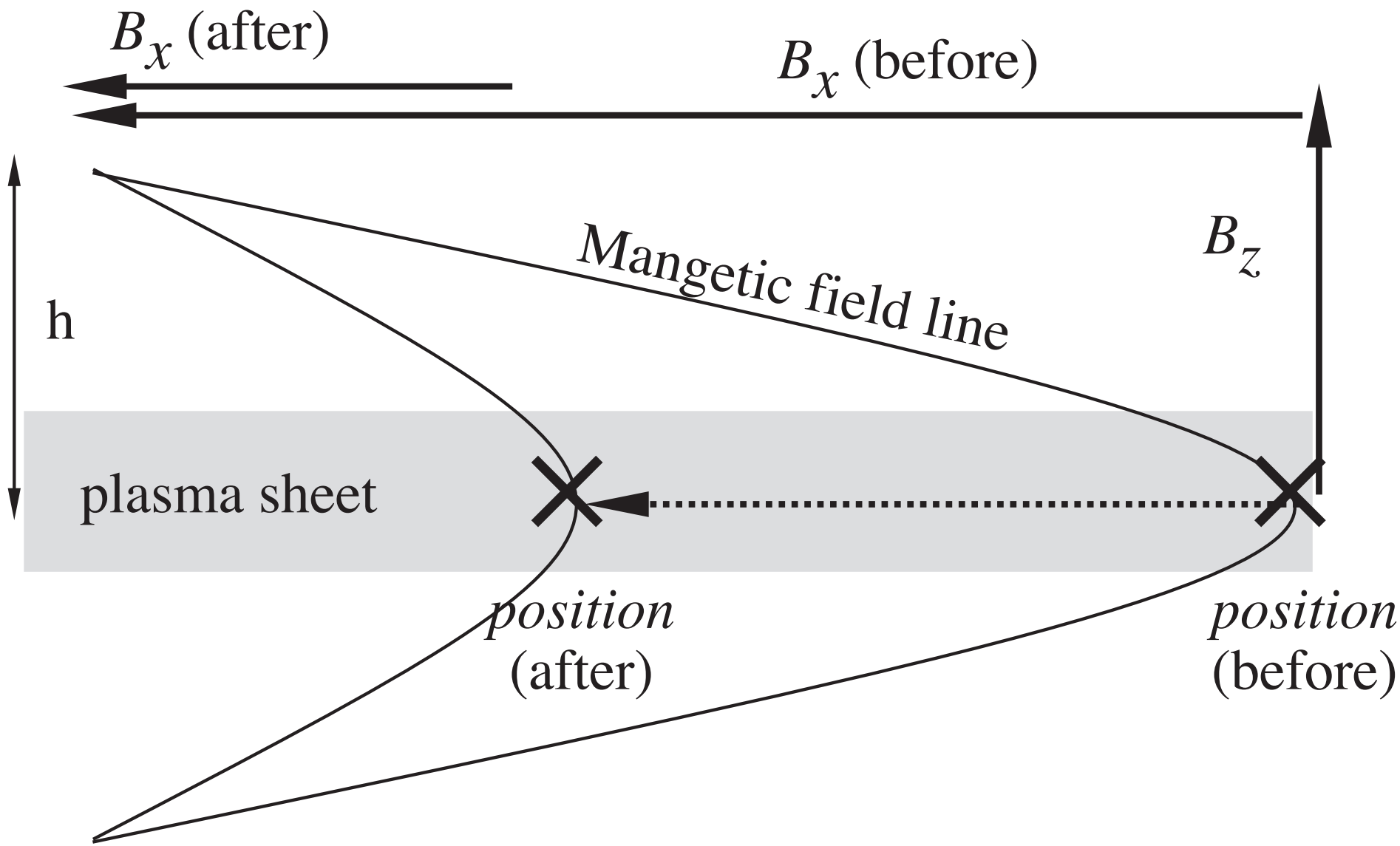
B_x (after)
B_x (before)
B_z
h
Mangetic field line
plasma sheet
position
(after)
position
(before)

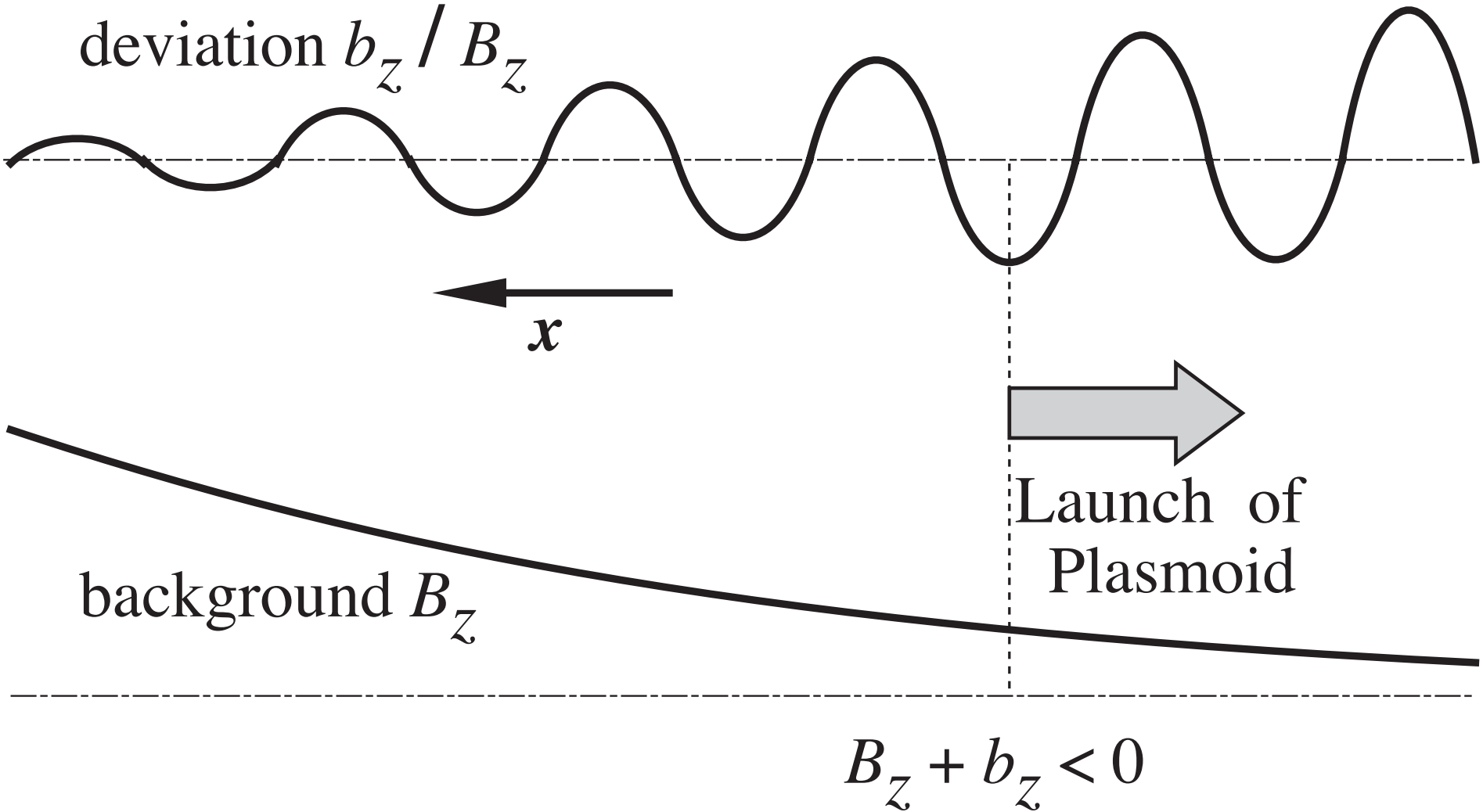
deviation b_z / B_z
x
Launch of Plasmoid
background B_z
$B_z + b_z < 0$